ELSEVIER

Contents lists available at ScienceDirect

## Journal of Biomechanics

journal homepage: www.elsevier.com/locate/jbiomech



# The influence of load carriage and prosthetic foot type on measures of biomechanical demand

Aude S. Lefranc <sup>a</sup>, Glenn K. Klute <sup>b,c</sup>, Richard R. Neptune <sup>a,\*</sup>

- <sup>a</sup> Walker Department of Mechanical Engineering, The University of Texas at Austin, Austin, TX, USA
- <sup>b</sup> Department of Veteran Affairs, Center for Limb Loss and MoBility, Seattle, WA, USA
- <sup>c</sup> Department of Mechanical Engineering, University of Washington, Seattle, WA, USA

#### ARTICLE INFO

#### Keywords: Lower limb amputation Load carriage Gait, Biomechanics Muscle function Modeling and simulation

#### ABSTRACT

Individuals with transtibial amputation (TTA) are at increased risk for conditions such as intact-limb osteoarthritis and fatigue, likely due to elevated joint loading and metabolic cost compared to unimpaired individuals. These risks are amplified during load carriage, as individuals with TTA lack residual limb ankle plantarflexors and rely more heavily on their intact limb to meet increased mechanical demands. This study used musculoskeletal modeling and simulation to evaluate how different prosthetic feet and load carriage positions affect biomechanical demand during steady-state walking. Measures included total metabolic cost, individual muscle contributions to metabolic cost, and intact limb axial knee joint impulses. Walking data were collected from five individuals with TTA across five loading conditions (no-load and 30 lbs. carried as a front-, back-, intact-side-, or residual-side-load) while wearing four prosthetic feet (a passive standard-of-care foot, a stiffer foot, a heelwedge-modified foot, and a dual-keel foot). Two participants also completed additional trials using a powered ankle-foot prosthesis. Front-load carriage resulted in the highest metabolic cost  $(7.56 \pm 0.40 \text{ W} * \text{kg}^{-1})$  while back-load carriage had the lowest (6.34  $\pm$  0.38 W \* kg $^{-1}$ ). Key contributors to increased metabolic cost included the gastrocnemius, soleus, gluteus maximus and gluteus medius. Front-load carriage had the lowest intact knee joint impulse (16.56  $\pm$  1.33 N \* s \* kg $^{-1}$ ) while intact-side-load carriage had the highest (20.60  $\pm$  1.39 N \* s \* kg<sup>-1</sup>). The optimal prosthetic foot varied greatly depending on load carriage position or biomechanical demand. These findings highlight the importance of tailoring both load carriage strategies and prosthetic foot prescriptions to the individual to optimize outcomes.

#### 1. Introduction

Individuals with a unilateral transtibial amputation (TTA) often experience altered gait mechanics including bilateral asymmetries (Sanderson & Martin, 1997), reduced walking speed (Robinson et al., 1987) and altered residual limb muscle activity (Winter & Sienko, 1988). Consequently, individuals with TTA are at increased risk of developing secondary disorders such as osteoarthritis in the intact limb and also tend to experience higher metabolic costs and fatigue compared to non-amputees (Burke et al., 1978; Gailey et al., 1994; Waters et al., 1976).

For non-amputees, carrying a load while walking results in significantly larger metabolic costs and increased heart rates relative to unloaded walking (Knapik et al., 2004; Quesada et al., 2000; Silder

et al., 2013). Further, load carriage results in increased peak ground reaction forces (GRFs), loading rates and joint loads (Polcyn et al., 2002; Silder et al., 2013), which have been associated with lower limb injuries and increased osteoarthritis risk (Baliunas et al., 2002; Grimston et al., 1991). Children and objects can be carried in different ways, but perhaps the most common methods include posteriorly in a backpack, anteriorly in a sling or with arms, or asymmetrically with arms on either side (Coleman et al., 2015; Knapik et al., 2004). While most load carriage studies have focused on the effects of a back load or a combined front and back load, the effects of side or front load carriage alone remain relatively unknown.

Load carriage during walking presents an even greater challenge for individuals with TTA due to the functional loss of the ankle plantarflexors. Passive energy storage and return (ESAR) feet have been

E-mail address: rneptune@mail.utexas.edu (R.R. Neptune).

<sup>\*</sup> Corresponding author at: Walker Department of Mechanical Engineering, The University of Texas at Austin, 204 E. Dean Keeton Street, Stop C2200, Austin, TX 78712-1591, USA.

designed with the intent of facilitating natural gait by seeking to replicate the biomechanical contributions of the ankle joint to tasks such as body support, forward propulsion and balance control. Clinicians typically prescribe the stiffness of ESAR feet based on an individual's anticipated activity level and body weight. While non-amputees modulate their ankle stiffness during loaded walking (Kern et al., 2019; Shamaei et al., 2013), the ESAR foot stiffness is constant and cannot adapt to accommodate load variations or as task demands change throughout the gait cycle. Thus, gradual weight changes often require refitting with a new prosthetic foot stiffness category, while sudden load changes lead to suboptimal stiffness. Clinicians have several low-cost options for individuals with TTA who routinely carry loads, including the prescription of a stiffer category foot, the addition of a heel wedge to stiffen the heel or the prescription of a dual keel prosthetic foot. During load carriage, a prosthetic foot with greater stiffness would be advantageous (Klodd et al., 2010); conversely, too high of a stiffness without a load is disadvantageous because it results in reduced energy storage and return (Fey et al., 2011). As a result, those using ESAR feet during altered load conditions experience greater metabolic cost, increased intact limb power generation and absorption, and increased prosthetic foot dorsiflexion during late stance (Doyle et al., 2014, 2015; Schnall et al., 2012, 2014).

Analysis of individual muscle and prosthetic ankle contributions to body support and forward propulsion using musculoskeletal modeling and simulation has demonstrated the importance of the ankle plantarflexors in maintaining a natural gait (Silverman & Neptune, 2012; Zmitrewicz et al., 2007). In addition, previous studies have highlighted the critical role of the ankle plantarflexors in maintaining balance control in both the frontal and sagittal planes (Neptune & McGowan, 2011, 2016) and adapting to altered load conditions (McGowan et al., 2008, 2009). Thus, a prosthesis that replicates ankle plantarflexor functionality would be advantageous in reducing biomechanical demand. While the potential benefits of powered-ankle prosthetic feet have been explored (Eilenberg et al., 2010; Herr & Grabowski, 2012; Montgomery & Grabowski, 2018; Sup et al., 2008), it is unclear whether those benefits translate to walking while carrying a load. Clinical trials examining prosthetic foot stiffness and damping have identified significant design trade-offs, with these parameters influencing biomechanical measures such as power generation, loading rate, and self-selected walking speed (Klute, 2023). However, the relationship between load carriage and commercially available prosthetic feet remains unclear.

The purpose of this study was to compare the effects of a range of passive and powered prosthetic feet on biomechanical measures of demand including metabolic cost and joint loading. In addition, the effects of load carriage position on these biomechanical quantities were evaluated for each prosthesis. This work is part of a broader investigation based on a shared dataset (Ardianuari et al., 2025; Lefranc et al., 2024). We anticipated that the feet which provided increased stiffness would result in reduced biomechanical demand relative to the standard-of-care foot during the loaded conditions, while the converse would be true during the unloaded condition. We also anticipated that the powered foot would result in the least biomechanical demand for all loading conditions. Further, we expected that one loading position would result in the least biomechanical demand, thereby being optimal relative to the other positions. Understanding the relationship between prosthetic foot

selection, load carriage position and these biomechanical measures of demand provides valuable insight into prosthetic foot prescription and design, as well as load carriage recommendations. This is essential to reducing fatigue, pain and the risk of developing comorbidities, which will ultimately improve amputee mobility and quality of life.

#### 2. Methods

#### 2.1. Data collection

Data were collected from five individuals (Table 1) with TTA walking at their self-selected walking speed (SSWS) across five overground force plates (AMTI), where the participants were instructed to walk in a straight line across the force plates. Trials were discarded and repeated if the participants were not walking within 10 % of their SSWS or if a trial did not have a single, complete foot contact on a force plate. Individuals were instructed to adjust their speed or starting point until all trials were close enough to their SSWS and each step was placed entirely on a force plate. Kinematic marker data were collected using a modified Plug-in-Gait full-model marker set consisting of sixty-two reflective markers and a 12-camera Vicon system. Electromyography (EMG) data were collected from 13 electrodes on key muscle groups (Lefranc et al., 2024). Twenty trials were collected for each individual, consisting of five loading conditions (no-load, front-load, back-load, intact-side-load and residual-side-load) while wearing four prosthetic feet (a passive clinically prescribed foot [PR], the same prescribed passive foot one category stiffer [SF], their prescribed foot with a heel stiffening wedge [HW] and a dual-keel foot [DK]; Fig. 1; (Klute, 2023)). Two participants also wore a powered ankle-foot prosthesis (PW; Empower, Ottobock) for all loading conditions, thus completing an additional five trials each. A 13.6 kg (30 lb) load was created using sand inside a cylindrical pack, which was placed inside a carrier (Ergobaby, Fig. 2) to be worn by participants. The subject was provided a minimum of 15 min to acclimate to each prosthesis/load combination. Rest breaks were provided as needed at the subject's request.

#### 2.2. Modeling and simulation framework

A generic 23-degree-of-freedom musculoskeletal model with 92 Hill-type musculotendon actuators (OpenSim model gait2392; Delp et al., 2007; Seth et al., 2018; Thelen, 2003) was modified to create a three-dimensional TTA model, as described in Lefranc et al. (2024). To model the various loading conditions, a 13.6 kg body was attached to the front, back, intact- and residual-side of the torso segment of the model with inertial properties adapted from Dembia et al. (2017). The interface between the mass and torso was modelled using a linear spring and damper along the vertical translational degrees of freedom. The spring constant and damping coefficient were adjusted for each subject and experimental condition so that the vertical pack translation closely matched that of the experimental kinematics (average values of  $k=5060 \ +/-468 \ N/m; \ b=319 \ +/-43 \ N \ * s/m).$ 

A representative gait cycle, defined as residual-side heel strike to subsequent residual-side heel strike, was identified from each trial. Simulations of each trial were performed using OpenSim 4.1 (Delp et al., 2007; Seth et al., 2018). Joint angles were determined using an inverse

**Table 1** Subject Demographics.

Subject	Age (years)	Sex	Height (mm)	Mass (kg)	Side of amputation	Time since amputation (Years)
1	40	Male	1799	101.5	Left	14
2	60	Male	1800	111.9	Right	3
3	39	Male	1712	105.7	Right	12
4	25	Female	1565	53.4	Right	24
5	43	Male	1820	107.0	Left	1
Mean $\pm$ standard deviation	$41\pm13$		$1739\pm106$	$96\pm24$		$11 \pm 9$

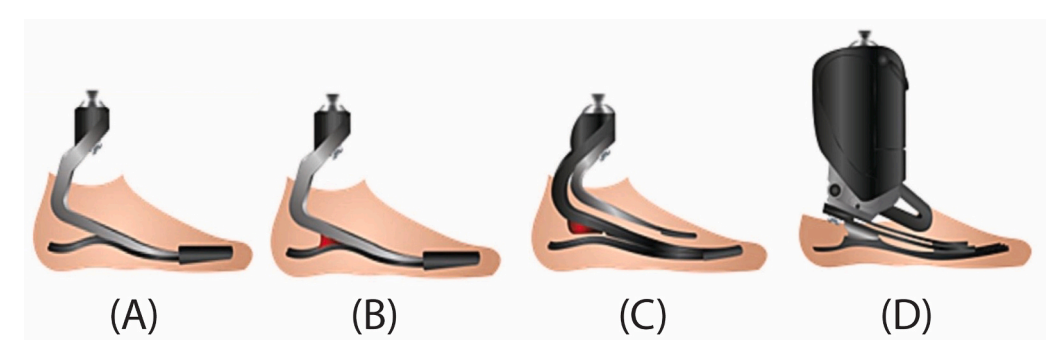


Fig. 1. Clinically prescribed foot and one category stiffer (A; PR, SF), Prescribed foot with heel-stiffening wedge (B; HW) Dual-keel foot (C; DK), and Powered ankle-foot (D; PW).

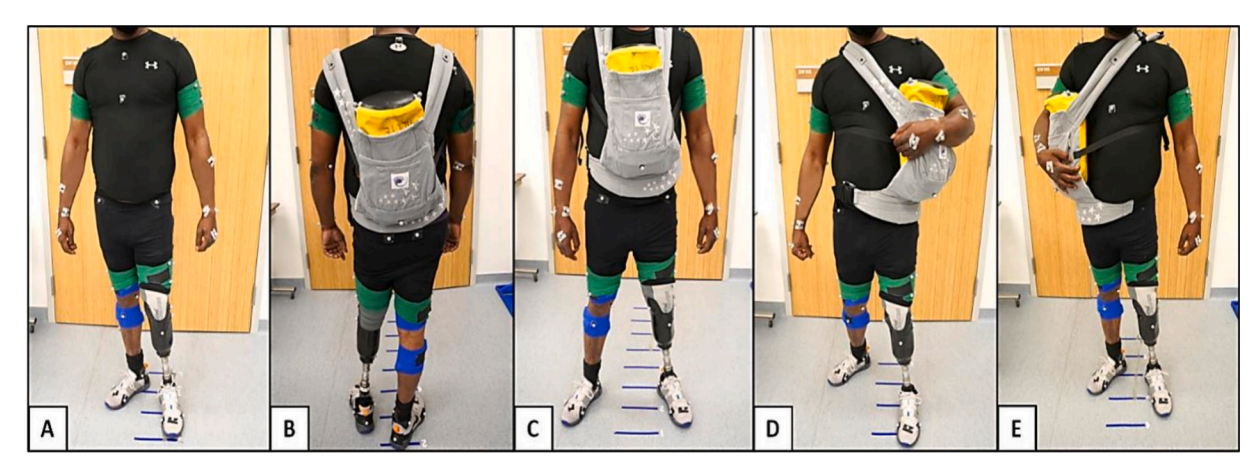


Fig. 2. (A) No-Load, (B) Back-Load, (C) Front-Load, (D) Residual-Side-Load, (E) Intact-Side-Load.

kinematics algorithm, which minimizes marker error between the experimental and model data. A residual reduction algorithm (RRA) was then used to adjust model mass properties and kinematics to ensure dynamic consistency between the GRFs and body segment kinematics. The resulting adjusted kinematics were used for all simulations. A computed muscle control algorithm (Thelen et al., 2003; Thelen and Anderson, 2006) was then used to determine the muscle excitations necessary to reproduce the kinematics obtained from RRA (Fig. 3). Each simulation was validated to confirm that the simulation muscle activations closely aligned with the EMG data, and that the kinematic errors, reserve actuators and residual forces were all within OpenSim's best

practices range (Hicks et al., 2015, Appendix).

#### 2.3. Measures of biomechanical demand

To estimate biomechanical demand, we analyzed metabolic cost and intact knee axial joint loads. To determine the metabolic cost, instantaneous metabolic power for each muscle was determined using the metabolic model by Umberger et al. (Uchida et al., 2016; Umberger, 2010; Umberger et al., 2003). Average metabolic power was calculated by integrating the instantaneous metabolic power  $(\dot{E})$  with respect to time over the gait cycle (Eq. (1)):

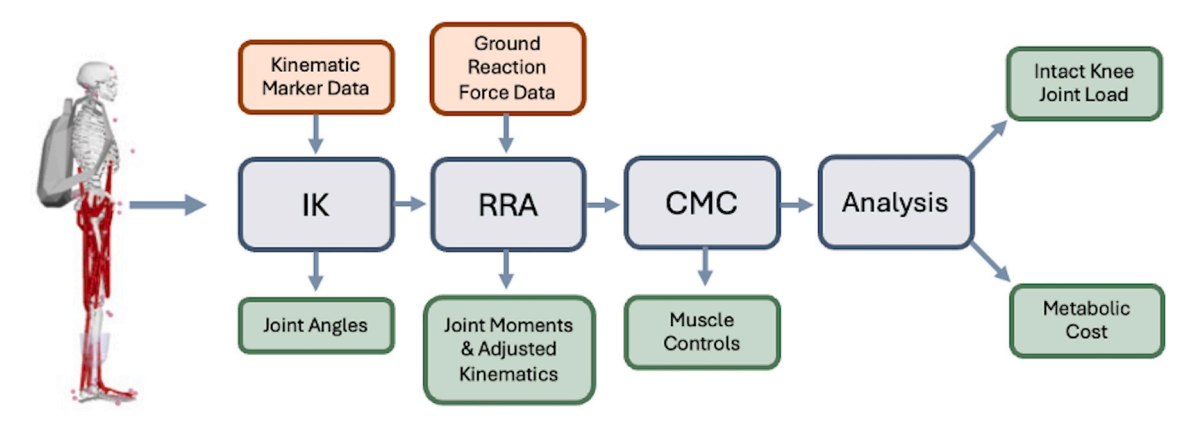


Fig. 3. Computational framework used to generate the simulations. Inverse kinematics (IK) was used to calculate joint angles from the experimental marker data. A residual reduction algorithm (RRA) reduced dynamic inconsistencies between GRFs and body segment kinematics by adjusting model mass properties and the kinematics. Computed muscle control (CMC) identified the muscle controls needed for the simulation to reproduce the experimental kinematics. Analyses were then performed to quantify the biomechanical demand measures of metabolic cost and intact knee joint loading.

$$E_{\rm gc} = \int_0^{t_{\rm g}} \dot{E}(t)dt \tag{1}$$

where  $t_g$  is the gait cycle time. Further, individual muscle contributions to metabolic power were determined by identifying the metabolic power generated by specific functional muscle groups (Table 2). Total average metabolic power (metabolic cost) was determined by summing the contributions from all the individual muscles in the model.

Intact knee axial joint loads were determined using OpenSim's joint reaction analysis tool, and then the joint contact impulse was calculated by time integrating the contact forces over the entire stance phase (Eq. (2):

$$J_{knee} = \int_0^{t_s} F_{knee}(t) dt \tag{2}$$

Both metabolic cost and joint contact impulse were normalized to body mass (no load condition) or body mass plus load.

#### 3. Results

#### 3.1. Total metabolic cost

As expected, the no-load condition resulted in the lowest metabolic cost across all prosthetic feet (5.9  $\pm$  0.3 W  $^{*}$  kg  $^{-1}$ ), followed by back (6.3  $\pm$  0.4 W  $^{*}$  kg  $^{-1}$ ), residual-side (6.8  $\pm$  0.4 W  $^{*}$  kg  $^{-1}$ ), intact-side (6.9  $\pm$  0.8 W  $^{*}$  kg  $^{-1}$ ), and front-load (7.6  $\pm$  0.4 W  $^{*}$  kg  $^{-1}$ ) conditions. The optimal loaded condition which resulted in the lowest metabolic cost was the back-load for the PR, DK and PW feet (6.0, 6.1 and 6.7 W  $^{*}$  kg  $^{-1}$ , respectively), the intact-side-load for the HW foot (5.7 W  $^{*}$  kg  $^{-1}$ ) and the residual-side-load for the SF foot (6.7 W  $^{*}$  kg  $^{-1}$ , Fig. 4). The PW foot had higher metabolic cost across all loading conditions compared to other feet.

#### 3.1.1. Individual muscle contributions to metabolic cost

The largest contributors to metabolic cost in both limbs were HAM, followed by GMAX, GAS, SOL and GMED (Figs. 5 and 6, Tables A1-2). The contributions of the intact- and residual-limb muscles to metabolic cost were often asymmetric, where the intact VAS (VASi) had a higher metabolic cost than the residual VAS (VAS<sub>r</sub>). Conversely, the HAM<sub>r</sub> contributed more to total metabolic cost than the HAM<sub>i</sub>. Relative to the no-load condition, HAM<sub>r</sub>, HAM<sub>i</sub>, RF<sub>r</sub> and RF<sub>i</sub> all responded to back-loads with reduced metabolic cost, while the other loading conditions, particularly the front-load, resulted in increased metabolic cost. GMAX, GMED<sub>i</sub>, VAS<sub>i</sub>, SOL, and GAS all had increased metabolic cost during loading; conversely, IL and VAS<sub>r</sub> were relatively unaffected by load carriage. The contribution of SOL and GAS to the metabolic cost increased more for the intact-side-loading condition than the residualside-loading condition, while the contribution of RF<sub>r</sub> increased more for the residual-side-load condition than the intact-side condition. For most muscles, the front-load condition resulted in the largest increase in metabolic cost.

**Table 2**Functional groups analyzed. Italicized muscles were not included in the residual limb of the amputee model.

Group	Muscles/actuators
FOOT	Prosthetic Foot
RF	Rectus Femoris
VAS	Vastus Medialis, Vastus Intermedius, Vastus Lateralis
GMAX	Superior, Middle and Inferior Gluteus Maximus
GMED	Anterior, Middle and Posterior Gluteus Medius and Minimus
HAM	Semimembranosus, Semitendinosus, Biceps Femoris Long Head, Gracilis
BFSH	Biceps Femoris Short Head
GAS	Medial Gastrocnemius, Lateral Gastrocnemius
SOL	Soleus, Tibialis Posterior, Flexor Digitorum Longus
TA	Tibialis Anterior, Extensor Digitorum Longus

The powered foot condition typically resulted in the greatest metabolic cost for most muscles across loading conditions, except VAS and  $\rm IL_i$  (Figs. 4–6). Further, relative to the PR foot, the SF foot consistently resulted in higher metabolic costs for most muscles, except for the frontload condition. The DK foot consistently produced higher metabolic costs in most muscles for the front-load condition compared to the other feet. The HW foot resulted in lower metabolic cost in both the intact- and residual-side muscles for the intact-side-load, while resulting in increased cost for the residual-side-load compared to the other feet.

#### 3.2. Axial intact knee joint impulses

As expected, the no-load condition resulted in the lowest average axial intact knee joint contact force impulses for all prostheses (Fig. 7). Of the loaded conditions, the intact-side-load resulted in the greatest intact knee impulses, followed by the residual-side-load, then the back-and front-loads. The front-load resulted in the smallest knee impulses for the DK, SF and HW feet (17.1, 14.7 and 15.3 N \* s \* kg $^{-1}$ , respectively), while the back-load resulted in the smallest knee impulses for the PW foot (16.7 N \* s \* kg $^{-1}$ ), and the residual-side-load resulted in the smallest impulse for the PR foot (15.9 N \* s \* kg $^{-1}$ ).

The best prosthesis for minimizing intact knee joint impulses was the PW foot for the no-load, back-load and intact-side-load conditions, the SF foot for the front-load condition and the PR foot for the residual-side-load condition (Fig. 7). Compared to the other feet, the HW foot resulted in relatively small knee impulses for the front- and back-loads (15.3 and 17.8 N \* s \* kg $^{-1}$ ), while resulting in relatively large impulses for the intact-side- and residual-side-loads (21.9 and 19.9 N \* s \* kg $^{-1}$ ). The SF foot produced relatively high joint impulses for all conditions besides the front-load condition, where it resulted in relatively small impulses. The PW foot resulted in consistent intact knee impulses across all loading conditions (17.7  $\pm$  0.8 N \* s \* kg $^{-1}$ ).

#### 4. Discussion

The results of this study indicate that the optimal prosthetic foot varies depending on loading position and measure of biomechanical demand (see Table 3). This suggests the need for patient-specific prescription as there was a large range of responses to each prosthetic foot. Increases in knee joint impulses resulting from a prosthetic foot or loading condition did not always correspond to increased metabolic cost, suggesting that variations in muscle coordination and walking mechanics caused these two measures of biomechanical demand to diverge. This also suggests that a prosthetic foot that is optimal for one metric may not be optimal for the other and foot prescription should be modified to target specific objectives.

The SF foot produced relatively high biomechanical demand for all conditions except during front-load carriage, suggesting that it may be detrimental for most prosthesis users, even under load-carriage conditions. We also found that the PW foot typically resulted in slightly lower intact knee impulses relative to the PR foot. Contrary to previous work (Esposito et al., 2016; Montgomery & Grabowski, 2018), the PW foot typically resulted in increased metabolic cost, particularly from HAM, RF and GMAX. Based on these outcomes, a standard PR foot may be advantageous in broadly reducing biomechanical demand, while a PW foot may be beneficial for those at risk of developing intact knee osteoarthritis.

While we observed a relationship between biomechanical demand and load position, the load position that was optimal for minimizing one measure of demand was not necessarily optimal for minimizing other measures. For individuals experiencing fatigue, carrying loads on their back may help minimize metabolic cost, while carrying a front-load may worsen fatigue. For individuals with intact knee pain or osteoarthritis, the results suggest that the front- and back-loading positions are optimal for reducing intact knee impulses, while carrying intact-side-loads may exacerbate knee pain.

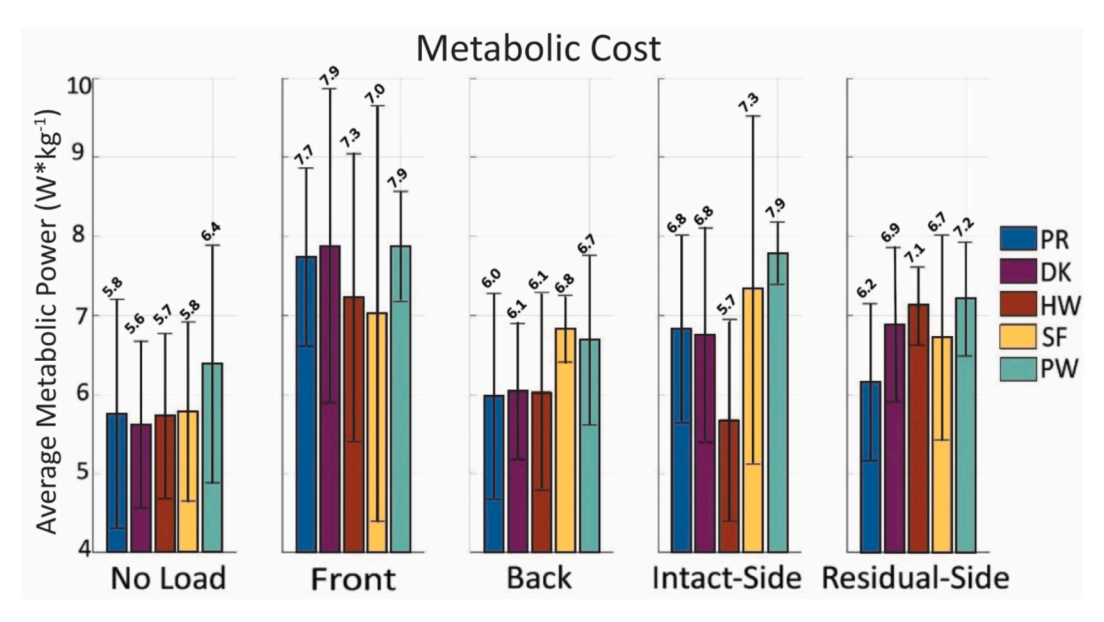


Fig. 4. Metabolic cost  $\pm$  one standard deviation across a gait cycle for five different loading conditions (unloaded, front, back, intact-side and residual-side loads). Prostheses evaluated include prescribed (PR), dual-keel (DK), prescribed with heel-wedge (HW), one category stiffer (SF) and Empower (Ottobock, Austin, TX) powered foot (PW).

#### 4.1. Metabolic cost

We found that all loading conditions required increased metabolic cost, consistent with previous work (Fallowfield et al., 2012; Schnall et al., 2012). Further, the front-load condition resulted in the greatest total metabolic cost, while the back-load condition resulted in the least. Previous studies have demonstrated the importance of the ankle plantarflexors (SOL and GAS) in producing the second vertical GRF peak and accelerating the COM during the second half of stance (Liu et al., 2006; McGowan et al., 2010; Neptune et al., 2001). In addition, GAS and SOL provide increased body support during load carriage (McGowan et al., 2010; Silder et al., 2013). Similarly, we found that the contributions to metabolic cost from GAS and SOL both increased in response to all loading conditions. Previous work has indicated that GMED and GMAX are primary contributors to load acceptance and body weight support during the first half of stance (McGowan et al., 2010), which is consistent with our results. Further, the participants demonstrated increased contributions from GMED; and GMAX; to metabolic cost relative to GMED<sub>r</sub> and GMAX<sub>r</sub>. These results suggest that individuals with TTA depend more heavily on their intact limb than their residual limb to accommodate increased loads.

We expected to see increased metabolic cost from HAM during the front-load condition and a reduced contribution to metabolic cost during the back-load condition, since HAM has been shown to be a key contributor to generating backward angular momentum in early stance (Neptune & McGowan, 2011). Indeed, HAM metabolic cost was greatest for the front-load condition and smallest for the back-load condition. Similarly, GMAX demonstrated increased metabolic cost during the front-load condition. This may reflect an attempt to increase muscle contributions to support, thus generating greater backwards angular momentum, which is consistent with a prior analysis using the same dataset (Lefranc et al., 2024). The increased metabolic cost from the hipextensors (GMAX and HAM) in combination with increased hip-flexor activity from RF suggests increased co-contraction at the hip during the front-load condition. Increased co-contraction is more commonly observed in individuals with orthopedic injuries or neuromuscular disorders to compensate for lack of joint stability (Higginson et al., 2006; Lamontagne et al., 2000; McGinnis et al., 2013; Rudolph et al., 2000). While co-contraction has been reported to increase joint stiffness and potentially leads to improved stability (Latash & Huang, 2015), it also results in increased metabolic cost (Moore et al., 2014). This suggests that individuals carrying front-loads may have increased perception of instability and may respond by stiffening their hip.

VAS metabolic cost was generally unaffected by load carriage, contrary to previous studies that found increased VAS activity in response to carrying a load (McGowan et al., 2010; Silder et al., 2013). However, Lefranc et al. (2024) found that VAS contributions to support and propulsion did not increase notably during load carriage, and therefore metabolic cost was relatively unchanged. These results suggest that the participants in the present study responded to load carriage by modulating other muscles rather than VAS.

We found that the PW foot did not reduce the metabolic cost. This result was consistent with some previous studies (e.g., Kim et al., 2021) but differed from others (e.g., Esposito et al., 2016; Herr & Grabowski, 2012). These discrepancies may be due to limited acclimatization time, suboptimal tuning of the prosthesis control algorithm, or differences in participant characteristics such as age and activity level. For instance, both Herr & Grabowski (2012) and Esposito et al. (2016) allowed for relatively long acclimatization periods (2 h and 3 weeks, respectively), and Esposito's participants were notably younger, with an average age of 29.

#### 4.2. Axial intact knee joint loads

Previous work has indicated that individuals with lower-limb amputations are at increased risk of developing intact knee osteoarthritis due to increased dependence and loading of their intact limb (Burke et al., 1978; Norvell et al., 2005; Struyf et al., 2009). The results of this study indicated that axial loading impulses in the intact knee were greater during load carriage than during the no-load condition, and specifically the intact-side-load condition produced the highest intact knee joint loads. Consequently, amputees who carry loads during activities of daily living, particularly on the intact-side, may be at an increased risk of developing intact knee pain and ultimately osteoarthritis (Burke et al., 1978; Norvell et al., 2005; Struyf et al., 2009).

These results appear to conflict with the findings of Ardianuari et al. (2025), who reported that the external knee adduction moment (KAM) on the intact limb was lowest during the intact-side-loading condition. While KAM serves as a proxy for medial compartment loading, it is highly sensitive to the direction of the GRFs relative to the knee joint

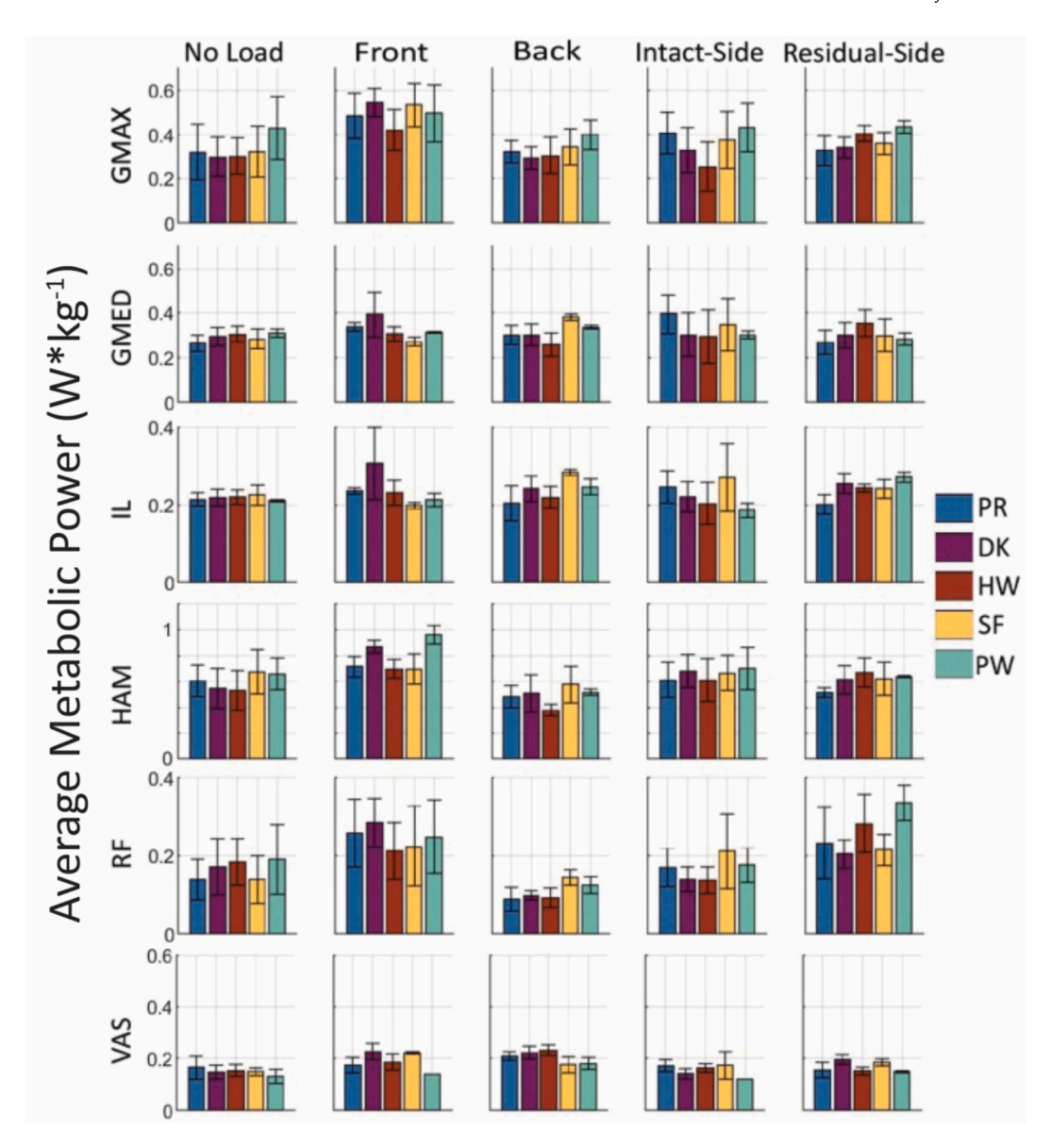


Fig. 5. Residual limb metabolic cost  $\pm$  one standard deviation across a gait cycle for GMAX, GMED, IL, HAM, RF and VAS across five different loading conditions (unloaded, front, back, intact-side and residual-side loads). Prostheses evaluated include prescribed (PR), dual-keel (DK), prescribed with heel-wedge (HW), one category stiffer (SF) and Empower (Ottobock, Austin, TX) powered foot (PW).

center and is not a direct measurement of total axial knee loading. Further, knee load estimates derived from musculoskeletal modeling capture the effects of compressive forces generated from muscles, providing a more comprehensive representation of joint loading.

Of the loaded conditions, the front-load condition had the lowest axial intact knee impulses for most prosthetic feet. Since GAS has been shown to be a primary contributor to knee joint loads (Sasaki & Neptune, 2010), reduced knee impulses may be due to reduced GAS contributions to support and propulsion, which is consistent with our previous findings (Lefranc et al., 2024).

The PW foot often resulted in the lowest intact knee impulses. Previous work has indicated that during early stance, VAS is the largest contributor to knee joint loads followed by RF (Sasaki & Neptune, 2010). Since the PW foot also resulted in reduced VAS contributions to metabolic cost, as well as reduced VAS and RF muscle contributions to support (Lefranc et al., 2024), VAS and RF are likely responsible for the reduced axial intact knee joint impulses observed in the PW foot.

#### 5. Conclusion

This study highlights the complex interaction between prosthetic foot type, load carriage position, and biomechanical demand in individuals with TTA. While the PR foot may offer broad benefits, the PW foot may better suit users concerned with intact knee loading. Similarly, back- and front-load positions may be preferred depending on whether metabolic efficiency or knee joint protection is prioritized. Patients prone to fatigue may benefit from back-load carriage, while those at risk of knee pain should avoid intact-side load carriage. These results emphasize that there is no universal optimal prosthetic foot, thus prescriptions should be individualized and tailored to each user's biomechanical needs and risk factors. Future prosthetic designs should incorporate adaptable stiffness that responds to activity, load carriage, and environmental demands.

#### 6. Limitations

Due to COVID-19-related challenges and the extensive nature of the

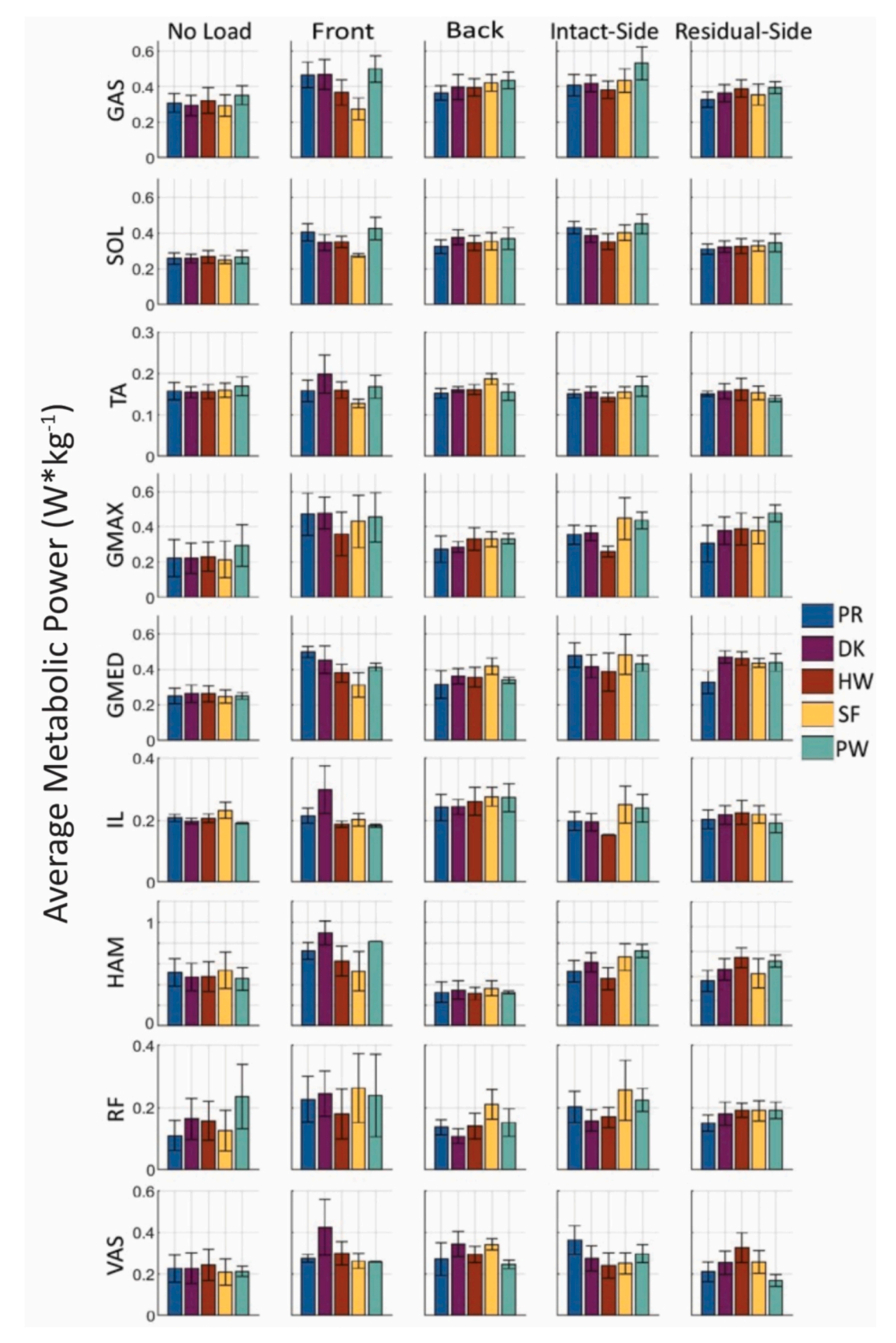


Fig. 6. Intact limb metabolic cost  $\pm$  one standard deviation across a gait cycle for GAS, SOL, TA, GMAX, GMED, IL, HAM, RF and VAS across five different loading conditions (unloaded, front, back, intact-side and residual-side loads). Prostheses evaluated include prescribed (PR), dual-keel (DK), prescribed with heel-wedge (HW), one category stiffer (SF) and Empower (Ottobock, Austin, TX) powered foot (PW).

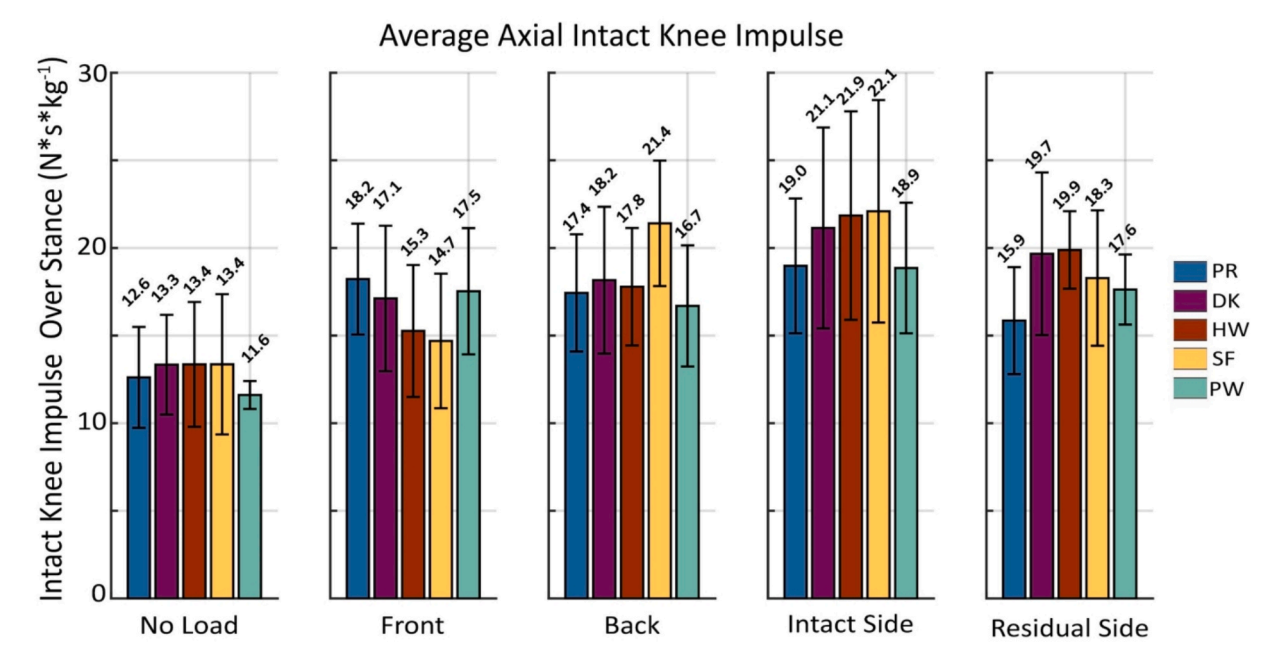


Fig. 7. Average axial intact knee impulses  $\pm$  one standard deviation across the stance phase of a gait cycle for five different loading conditions (unloaded, front, back, intact-side and residual-side loads). Prostheses evaluated include prescribed (PR), dual-keel (DK), prescribed with heel-wedge (HW), one category stiffer (SF) and Empower (Ottobock, Austin, TX) powered foot (PW).

# Table 3 Prosthetic foot which performed the best for each load carriage position and measure of biomechanical demand. Feet evaluated included a clinically prescribed energy-storage and return foot (PR), a one-category stiffer than prescribed foot (SF), a dual-keel foot (DK), a prescribed foot with a heel-stiffening wedge (HW) and a powered-ankle prosthetic foot (PW).

	No- load	Front- load	Back- load	Intact-side- load	Residual-side- load
Metabolic cost	DK	SF	PR	HW	PR
Axial intact knee	PW	SF	PW	PW	PR

protocol, recruiting participants who could safely complete the study was difficult, resulting in below-target enrollment. Further, due to the build height of the PW foot, most participants did not have enough pylon length to use the PW foot, so data were only collected from two participants. Further research with more participants is recommended to generalize the findings. For further discussion of limitations related to sample size, acclimation, data collection and modeling, please see Lefranc et al. (2024).

### Appendix

#### CRediT authorship contribution statement

Aude S. Lefranc: Writing – original draft, Visualization, Validation, Software, Investigation, Formal analysis. Glenn K. Klute: Writing – review & editing, Project administration, Methodology, Investigation, Funding acquisition, Data curation, Conceptualization. Richard R. Neptune: Writing – review & editing, Supervision, Resources, Project administration, Methodology, Investigation, Funding acquisition, Conceptualization.

#### Declaration of competing interest

The authors declare that they have no known competing financial interests or personal relationships that could have appeared to influence the work reported in this paper.

#### Acknowledgements

This research was supported in part by awards IO1 RX003138 and IK6 RX002974 from the United States Department of Veterans Affairs Rehabilitation Research, Development and Translation.

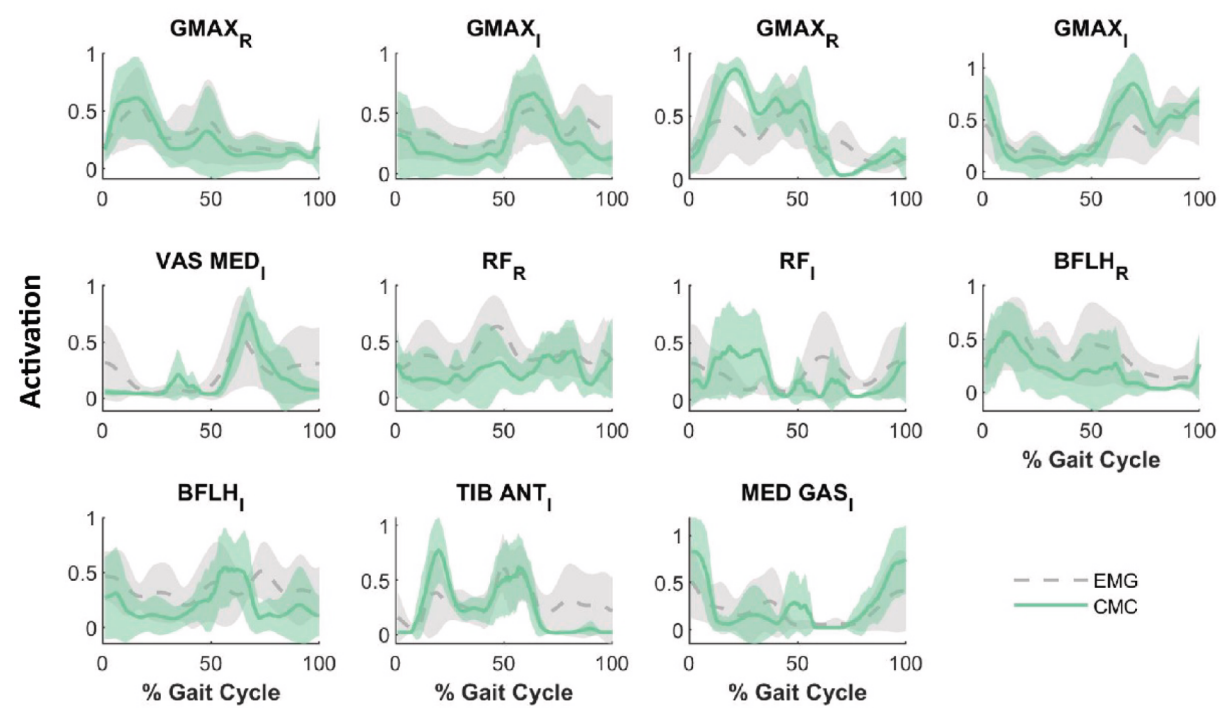


Fig. A1. Normalized CMC-derived muscle activation patterns (solid line) compared to electromyography (EMG) data (dashed line) averaged across all participants walking with no load with their prescribed foot. Shaded regions represent  $\pm$  1 standard deviation.

Table A1 Means and standard deviations for individual muscle contributions to metabolic cost in the residual limb (N \* s \* kg $^{-1}$ ).

Group	Foot	No load	Front	Back	Intact-side	Residual-side
$GMAX_r$	PR	$0.32 \pm 0.13$	$0.48 \pm 0.10$	$0.31\pm0.06$	$0.41\pm0.09$	$0.35\pm0.05$
	DK	$0.30\pm0.09$	$0.54\pm0.06$	$0.30\pm0.05$	$0.33\pm0.10$	$0.34 \pm 0.05$
	HW	$0.30\pm0.08$	$0.42\pm0.09$	$0.31\pm0.08$	$0.26\pm0.11$	$0.41\pm0.04$
	SF	$0.32 \pm 0.11$	$0.53\pm0.10$	$0.35\pm0.08$	$0.38\pm0.13$	$0.36\pm0.05$
	PW	$0.43 \pm 0.12$	$0.50\pm0.13$	$0.40\pm0.07$	$0.43 \pm 0.11$	$0.43\pm0.03$
$GMED_r$	PR	$0.26\pm0.04$	$0.34 \pm 0.02$	$0.33 \pm 0.04$	$0.40\pm0.09$	$0.24\pm0.04$
GMLDI	DK	$0.30 \pm 0.04$	$0.39 \pm 0.10$	$0.30 \pm 0.05$	$0.30 \pm 0.10$	$0.30 \pm 0.06$
	HW	$0.31 \pm 0.03$	$0.31 \pm 0.03$	$0.26 \pm 0.05$	$0.29 \pm 0.12$	$0.35 \pm 0.06$
	SF	$0.28 \pm 0.05$	$0.27 \pm 0.02$	$0.38 \pm 0.01$	$0.35 \pm 0.12$	$0.30 \pm 0.07$
	PW	$0.31\pm0.02$	$0.31 \pm 0.00$	$0.34 \pm 0.01$	$0.30\pm0.02$	$0.28\pm0.03$
11	PR	$0.21 \pm 0.02$	$0.24 \pm 0.01$	$0.21 \pm 0.04$	$0.25\pm0.04$	$0.19 \pm 0.04$
$IL_r$	DK	$0.21 \pm 0.02$ $0.22 \pm 0.02$	$0.24 \pm 0.01$ $0.31 \pm 0.09$	$0.21 \pm 0.04$ $0.24 \pm 0.03$	$0.25 \pm 0.04$ $0.22 \pm 0.04$	$0.19 \pm 0.04$ $0.25 \pm 0.03$
	HW	$0.22 \pm 0.02$ $0.22 \pm 0.02$	$0.31 \pm 0.09$ $0.23 \pm 0.03$	$0.24 \pm 0.03$ $0.22 \pm 0.03$	$0.22 \pm 0.04$ $0.20 \pm 0.05$	$0.23 \pm 0.03$ $0.24 \pm 0.01$
	SF	$0.22 \pm 0.02$ $0.23 \pm 0.03$	$0.20 \pm 0.03$ $0.20 \pm 0.01$	$0.22 \pm 0.03$ $0.28 \pm 0.01$	$0.20 \pm 0.03$ $0.27 \pm 0.09$	$0.24 \pm 0.01$ $0.24 \pm 0.02$
	PW	$0.23 \pm 0.03$ $0.21 \pm 0.00$	$0.20 \pm 0.01$ $0.21 \pm 0.02$	$0.25 \pm 0.01$ $0.25 \pm 0.02$	$0.27 \pm 0.09$ $0.19 \pm 0.02$	$0.24 \pm 0.02$ $0.27 \pm 0.01$
	1 **	0.21 ± 0.00	0.21 ± 0.02	0.25 ± 0.02	0.17 ± 0.02	0.27 ± 0.01
$HAM_r$	PR	$0.61 \pm 0.12$	$0.71\pm0.08$	$0.48 \pm 0.09$	$0.62 \pm 0.13$	$\textbf{0.54} \pm \textbf{0.03}$
	DK	$0.55\pm0.14$	$0.87\pm0.05$	$0.51\pm0.15$	$0.68 \pm 0.13$	$0.62\pm0.11$
	HW	$0.53\pm0.15$	$0.70\pm0.07$	$0.38\pm0.05$	$0.61\pm0.17$	$0.67\pm0.11$
	SF	$0.68\pm0.18$	$0.70\pm0.11$	$0.58\pm0.14$	$0.67\pm0.13$	$0.62\pm0.13$
	PW	$0.66\pm0.12$	$0.96\pm0.07$	$0.52\pm0.03$	$0.70\pm0.17$	$0.64 \pm 0.01$
$RF_r$	PR	$0.14 \pm 0.05$	$0.26\pm0.09$	$0.09 \pm 0.03$	$0.17 \pm 0.05$	$0.23\pm0.10$
-	DK	$0.17\pm0.07$	$0.29 \pm 0.06$	$0.10\pm0.01$	$0.14\pm0.03$	$0.20\pm0.04$
	HW	$0.18 \pm 0.06$	$0.21\pm0.07$	$0.09 \pm 0.02$	$0.14\pm0.03$	$0.28 \pm 0.07$
	SF	$0.14 \pm 0.06$	$0.23\pm0.10$	$0.14\pm0.02$	$0.21\pm0.10$	$0.22 \pm 0.04$
	PW	$0.19 \pm 0.09$	$0.25\pm0.09$	$0.12\pm0.02$	$0.18\pm0.04$	$0.34 \pm 0.04$
VAS <sub>r</sub>	PR	$0.17 \pm 0.04$	$0.17 \pm 0.03$	$0.18 \pm 0.03$	$0.17 \pm 0.02$	$0.19 \pm 0.03$
• 110 <sub>T</sub>	DK	$0.17 \pm 0.04$ $0.15 \pm 0.03$	$0.17 \pm 0.03$ $0.23 \pm 0.03$	$0.10 \pm 0.03$ $0.22 \pm 0.03$	$0.17 \pm 0.02$ $0.14 \pm 0.02$	$0.19 \pm 0.03$ $0.19 \pm 0.02$
	HW	$0.15 \pm 0.03$ $0.15 \pm 0.02$	$0.19 \pm 0.03$	$0.22 \pm 0.03$ $0.23 \pm 0.02$	$0.14 \pm 0.02$ $0.16 \pm 0.02$	$0.15 \pm 0.02$ $0.15 \pm 0.01$
	SF	$0.15 \pm 0.02$ $0.15 \pm 0.01$	$0.17 \pm 0.03$ $0.22 \pm 0.01$	$0.18 \pm 0.03$	$0.10 \pm 0.02$ $0.17 \pm 0.05$	$0.13 \pm 0.01$ $0.18 \pm 0.01$
	PW	$0.13 \pm 0.01$ $0.13 \pm 0.03$	$0.14 \pm 0.00$	$0.18 \pm 0.03$ $0.18 \pm 0.02$	$0.17 \pm 0.03$ $0.12 \pm 0.00$	$0.15 \pm 0.01$ $0.15 \pm 0.00$
	. "	0.10 ± 0.00	0.1 . ± 0.00	0.10 ± 0.02	5.12 ± 0.00	3.10 ± 0.00

 $\begin{tabular}{ll} \textbf{Table A2} \\ \textbf{Means and standard deviations for individual muscle contributions to metabolic cost in the intact limb (N * s * kg$^{-1}$).} \\ \end{tabular}$ 

Foot	No Load	Front	Back	Intact-Side	Residual-Side
PR	$0.31 \pm 0.05$	$0.47\pm0.07$	$0.36 \pm 0.04$	$0.41 \pm 0.06$	$0.34 \pm 0.04$
DK	$0.29 \pm 0.06$	$0.47\pm0.08$	$0.40\pm0.07$	$0.42\pm0.05$	$0.36\pm0.05$
HW	$0.32\pm0.07$	$0.37\pm0.07$	$0.40\pm0.05$	$0.38\pm0.05$	$0.39\pm0.05$
SF	$0.29\pm0.06$	$0.27\pm0.06$	$0.42\pm0.05$	$0.43\pm0.07$	$0.36\pm0.06$
PW	$0.35\pm0.05$	$0.50\pm0.07$	$0.43\pm0.05$	$0.53\pm0.10$	$0.40\pm0.03$
DD.	0.06 + 0.00	0.40   0.05	0.00 + 0.04	0.40   0.00	0.00 + 0.00
					$0.32 \pm 0.03$
					$0.32 \pm 0.03$
					$0.33 \pm 0.04$
PW	$0.25 \pm 0.02$ $0.26 \pm 0.04$	$0.27 \pm 0.01$ $0.43 \pm 0.06$	$0.35 \pm 0.05$ $0.37 \pm 0.06$	$0.40 \pm 0.04$ $0.45 \pm 0.05$	$\begin{array}{c} 0.33 \pm 0.03 \\ 0.34 \pm 0.05 \end{array}$
PR	$0.16\pm0.02$	$0.16\pm0.03$	$0.16\pm0.01$	$0.15\pm0.01$	$0.15\pm0.01$
DK					$0.16\pm0.02$
HW	$0.16\pm0.02$	$0.16\pm0.02$	$0.16\pm0.01$	$0.14\pm0.01$	$0.16\pm0.03$
SF	$0.16\pm0.02$	$0.13\pm0.01$	$0.19 \pm 0.01$	$0.15\pm0.01$	$0.15\pm0.02$
PW	$0.17\pm0.02$	$0.17\pm0.03$	$0.15\pm0.02$	$0.17 \pm 0.02$	$0.14\pm0.01$
					$0.30\pm0.11$
					$0.38 \pm 0.08$
					$0.39 \pm 0.09$
					$0.38 \pm 0.07$
PW	$0.29 \pm 0.12$	$0.45 \pm 0.14$	$0.33\pm0.03$	$0.43\pm0.05$	$0.48\pm0.05$
PR	$0.25 \pm 0.04$	$0.50 \pm 0.03$	$0.33 \pm 0.07$	$0.48 \pm 0.07$	$0.32 \pm 0.07$
					$0.47 \pm 0.03$
					$0.46 \pm 0.04$
					$0.44 \pm 0.02$
PW	$0.25 \pm 0.02$	$0.41 \pm 0.02$	$0.34 \pm 0.02$	$0.43 \pm 0.05$	$0.44 \pm 0.05$
					$0.17\pm0.02$
					$0.22\pm0.03$
					$0.22\pm0.04$
SF	$0.23\pm0.02$	$0.20\pm0.02$	$0.27\pm0.03$	$0.25\pm0.06$	$0.22\pm0.03$
PW	$0.19\pm0.00$	$0.18\pm0.00$	$0.27\pm0.04$	$0.24\pm0.04$	$0.19\pm0.03$
PR	$0.52 \pm 0.13$	$0.72 \pm 0.08$	$0.34 \pm 0.09$	$0.53 \pm 0.10$	$0.35 \pm 0.09$
					$0.46 \pm 0.09$
					$0.55 \pm 0.08$
					$0.33 \pm 0.08$ $0.42 \pm 0.12$
					$0.42 \pm 0.12$ $0.52 \pm 0.05$
1 11	0.10 ± 0.11	0.02 ± 0.00	0.00 ± 0.02	0.72 ± 0.00	0.02 ± 0.00
PR	$0.11\pm0.05$	$\textbf{0.23} \pm \textbf{0.07}$	$0.13 \pm 0.03$	$0.20\pm0.05$	$0.15\pm0.03$
	$0.16\pm0.07$		$0.11\pm0.02$		$0.18\pm0.04$
HW	$0.16\pm0.06$	$0.18\pm0.08$	$0.14\pm0.04$	$0.17\pm0.03$	$0.19\pm0.02$
SF	$0.13\pm0.06$	$0.26\pm0.11$	$0.21\pm0.05$	$0.26\pm0.10$	$0.19\pm0.03$
PW	$0.24\pm0.10$	$0.24 \pm 0.13$	$0.15\pm0.04$	$0.22\pm0.04$	$0.19\pm0.03$
DR	$0.23 \pm 0.07$	0.28 ± 0.02	$0.28 \pm 0.07$	0.36 ± 0.07	$0.20\pm0.06$
					$0.20 \pm 0.06$ $0.25 \pm 0.06$
					$0.25 \pm 0.06$ $0.33 \pm 0.07$
					$0.33 \pm 0.07$ $0.26 \pm 0.05$
PW	$0.21 \pm 0.03$	$0.20 \pm 0.00$	$0.25 \pm 0.02$	$0.30 \pm 0.04$	$0.17 \pm 0.03$
	PR DK HW SF PW  PR DK HW SF PW	$\begin{array}{cccccccccccccccccccccccccccccccccccc$	$\begin{array}{cccccccccccccccccccccccccccccccccccc$	$\begin{array}{c} \text{PR} & 0.31 \pm 0.05 \\ \text{DK} & 0.29 \pm 0.06 \\ \text{DK} & 0.29 \pm 0.06 \\ \text{DM} & 0.37 \pm 0.07 \\ \text{OM} & 0.40 \pm 0.07 \\ \text{SF} & 0.29 \pm 0.06 \\ \text{OM} & 0.35 \pm 0.05 \\ \text{OSD} & 0.50 \pm 0.07 \\ \text{OM} & 0.35 \pm 0.05 \\ \text{DW} & 0.35 \pm 0.05 \\ \text{OSD} & 0.50 \pm 0.07 \\ \text{OM} & 0.42 \pm 0.05 \\ \text{DW} & 0.35 \pm 0.05 \\ \text{OSD} & 0.50 \pm 0.07 \\ \text{DW} & 0.35 \pm 0.05 \\ \text{DN} & 0.26 \pm 0.02 \\ \text{DN} & 0.26 \pm 0.02 \\ \text{OM} & 0.33 \pm 0.03 \\ \text{DN} & 0.26 \pm 0.02 \\ \text{OM} & 0.35 \pm 0.05 \\ \text{OM} & 0.38 \pm 0.04 \\ \text{HW} & 0.27 \pm 0.03 \\ \text{SF} & 0.25 \pm 0.02 \\ \text{OM} & 0.26 \pm 0.04 \\ \text{DM} & 0.37 \pm 0.06 \\ \text{DW} & 0.26 \pm 0.04 \\ \text{DM} & 0.37 \pm 0.06 \\ \text{DW} & 0.26 \pm 0.04 \\ \text{DM} & 0.16 \pm 0.02 \\ \text{DM} & 0.17 \pm 0.02 \\ \text{DM} & 0.22 \pm 0.08 \\ \text{DM} & 0.37 \pm 0.06 \\ \text{DM} & 0.22 \pm 0.08 \\ \text{DM} & 0.32 \pm 0.06 \\ \text{DM} & 0.22 \pm 0.08 \\ \text{DM} & 0.32 \pm 0.06 \\ \text{DM} & 0.29 \pm 0.12 \\ \text{DM} & 0.29 \pm 0.12 \\ \text{DM} & 0.26 \pm 0.04 \\ \text{DM} & 0.26 \pm 0.05 \\ \text{DM} & 0.26 \pm 0.04 \\ \text{DM} & 0.36 \pm 0.05 \\ \text{DM} & 0.26 \pm 0.05 \\ \text{DM} & 0.36 \pm 0.06 \\ \text{DM} & 0.36$	$\begin{array}{c} PR & 0.31 \pm 0.05 & 0.47 \pm 0.07 & 0.36 \pm 0.04 & 0.41 \pm 0.06 \\ DK & 0.29 \pm 0.06 & 0.47 \pm 0.08 & 0.40 \pm 0.07 & 0.42 \pm 0.05 \\ DK & 0.29 \pm 0.06 & 0.47 \pm 0.08 & 0.40 \pm 0.07 & 0.42 \pm 0.05 \\ SF & 0.29 \pm 0.06 & 0.27 \pm 0.06 & 0.42 \pm 0.05 & 0.43 \pm 0.05 \\ PW & 0.55 \pm 0.05 & 0.50 \pm 0.07 & 0.43 \pm 0.05 & 0.53 \pm 0.10 \\ PR & 0.26 \pm 0.03 & 0.40 \pm 0.05 & 0.33 \pm 0.04 & 0.43 \pm 0.03 \\ DK & 0.26 \pm 0.02 & 0.35 \pm 0.05 & 0.33 \pm 0.04 & 0.43 \pm 0.03 \\ DK & 0.26 \pm 0.02 & 0.35 \pm 0.05 & 0.33 \pm 0.04 & 0.38 \pm 0.04 \\ HW & 0.27 \pm 0.03 & 0.35 \pm 0.03 & 0.34 \pm 0.04 & 0.38 \pm 0.04 \\ SF & 0.25 \pm 0.02 & 0.27 \pm 0.01 & 0.35 \pm 0.05 & 0.34 \pm 0.04 & 0.35 \pm 0.04 \\ PW & 0.26 \pm 0.02 & 0.27 \pm 0.01 & 0.35 \pm 0.05 & 0.40 \pm 0.05 \\ PR & 0.16 \pm 0.02 & 0.16 \pm 0.03 & 0.16 \pm 0.01 & 0.15 \pm 0.01 \\ DK & 0.15 \pm 0.01 & 0.20 \pm 0.05 & 0.16 \pm 0.01 & 0.15 \pm 0.01 \\ HW & 0.16 \pm 0.02 & 0.16 \pm 0.02 & 0.16 \pm 0.02 & 0.16 \pm 0.01 & 0.15 \pm 0.01 \\ PW & 0.17 \pm 0.02 & 0.17 \pm 0.03 & 0.15 \pm 0.02 & 0.17 \pm 0.03 \\ PR & 0.22 \pm 0.11 & 0.47 \pm 0.12 & 0.28 \pm 0.07 & 0.35 \pm 0.06 \\ DK & 0.15 \pm 0.01 & 0.17 \pm 0.03 & 0.15 \pm 0.02 & 0.17 \pm 0.02 \\ PR & 0.22 \pm 0.18 & 0.48 \pm 0.09 & 0.28 \pm 0.07 & 0.35 \pm 0.06 \\ DK & 0.22 \pm 0.08 & 0.48 \pm 0.09 & 0.28 \pm 0.03 & 0.36 \pm 0.04 \\ PW & 0.23 \pm 0.08 & 0.48 \pm 0.09 & 0.28 \pm 0.03 & 0.36 \pm 0.04 \\ PW & 0.23 \pm 0.08 & 0.48 \pm 0.09 & 0.28 \pm 0.03 & 0.36 \pm 0.04 \\ PW & 0.23 \pm 0.08 & 0.48 \pm 0.09 & 0.28 \pm 0.03 & 0.36 \pm 0.04 \\ PW & 0.23 \pm 0.04 & 0.50 \pm 0.03 & 0.33 \pm 0.04 & 0.45 \pm 0.12 \\ DK & 0.25 \pm 0.04 & 0.50 \pm 0.03 & 0.33 \pm 0.04 & 0.45 \pm 0.12 \\ DK & 0.25 \pm 0.04 & 0.50 \pm 0.03 & 0.33 \pm 0.04 & 0.44 \pm 0.05 \\ PW & 0.29 \pm 0.12 & 0.45 \pm 0.14 & 0.33 \pm 0.05 & 0.38 \pm 0.04 \\ PW & 0.25 \pm 0.04 & 0.31 \pm 0.05 & 0.33 \pm 0.04 & 0.42 \pm 0.06 \\ PW & 0.29 \pm 0.12 & 0.45 \pm 0.14 & 0.33 \pm 0.05 & 0.38 \pm 0.04 \\ PW & 0.25 \pm 0.04 & 0.31 \pm 0.05 & 0.33 \pm 0.04 & 0.42 \pm 0.06 \\ PW & 0.29 \pm 0.01 & 0.19 \pm 0.01 & 0.20 \pm 0.03 & 0.36 \pm 0.04 \\ PW & 0.25 \pm 0.04 & 0.31 \pm 0.05 & 0.33 \pm 0.04 & 0.42 \pm 0.05 \\ PW & 0.29 \pm 0.04 & 0.31 $

Table A3 Marker root mean squared (RMS) and standard deviation (STD) kinematic errors (cm, deg) across all participants for model scaling and inverse kinematics (IK) steps.

	Scaling and IK	
	RMS	STD
Scaling Marker Errors (cm)	0.82	0.09
IK Marker Errors (cm)	1.62	0.24

#### Table A4

Marker root mean squared (RMS) and standard deviation (STD) kinematic errors (cm, deg), residual forces (N), and residual moments ( $N^*m$ ) across all participants for residual reduction algorithm (RRA) step.

	RRA		
	RMS	STD	
RRA Trans (cm)	0.41	0.22	
RRA Rot (deg)	0.11	0.06	
Residual Forces (N)	5.08	2.98	
Residual Moments (N*m)	10.12	4.38	

#### Table A5

Marker root mean squared (RMS) and standard deviation (STD) kinematic errors (cm, deg), residual forces (N), residual moments (N  $^{*}$  m) and reserve actuator moments (N $^{*}$ m) across all participants and conditions for CMC step.

	CMC		
	RMS	STD	
CMC Trans (cm)	0.02	0.01	
CMC Rot (deg)	0.27	0.13	
Residual Forces (N)	4.80	2.77	
Residual Moments (N * m)	19.29	9.00	
Reserves Actuators (N * m)	4.94	3.29	

#### References

- Ardianuari, S., Morgenroth, D.C., Neptune, R.R., Klute, G.K., 2025. Load carriage influences intact limb knee loading estimate associated with osteoarthritis in individuals with transtibial amputation. Clin. Biomech. 124, 106486. https://doi. org/10.1016/j.clinbiomech.2025.106486.
- Baliunas, A.J., Hurwitz, D.E., Ryals, A.B., Karrar, A., Case, J.P., Block, J.A., Andriacchi, T.P., 2002. Increased knee joint loads during walking are present in subjects with knee osteoarthritis. Osteoarthr. Cartil. 10 (7), 573–579. https://doi. org/10.1053/joca.2002.0797.
- Burke, M.J., Roman, V., Wright, V., 1978. Bone and joint changes in lower limb amputees. Ann. Rheum. Dis. 37 (3), 252–254. https://doi.org/10.1136/ard.37.3.252.
- Coleman, T.J., Hamad, N.M., Shaw, J.M., Egger, M.J., Hsu, Y., Hitchcock, R., Jin, H., Choi, C.K., Nygaard, I.E., 2015. Effects of walking speeds and carrying techniques on intra-abdominal pressure in women. Int. Urogynecol. J. 26 (7), 967–974. https:// doi.org/10.1007/s00192-014-2593-5.
- Delp, S.L., Anderson, F.C., Arnold, A.S., Loan, P., Habib, A., John, C.T., Guendelman, E., Thelen, D.G., 2007. OpenSim: Open-source software to create and analyze dynamic simulations of movement. IEEE Trans. Biomed. Eng. 54 (11), 1940–1950. https:// doi.org/10.1109/TBMF.2007.901024.
- Dembia, C.L., Silder, A., Uchida, T.K., Hicks, J.L., Delp, S.L., 2017. Simulating ideal assistive devices to reduce the metabolic cost of walking with heavy loads. PLoS One 12 (7). https://doi.org/10.1371/journal.pone.0180320.
- Doyle, S.S., Lemaire, E.D., Besemann, M., Dudek, N.L., 2014. Changes to level ground transtibial amputee gait with a weighted backpack. Clin. Biomech. 29 (2), 149–154. https://doi.org/10.1016/j.clinbiomech.2013.11.019.
- Doyle, S.S., Lemaire, E.D., Besemann, M., Dudek, N.L., 2015. Changes to transtibial amputee gait with a weighted backpack on multiple surfaces. Clin. Biomech. 30 (10), 1119–1124. https://doi.org/10.1016/j.clinbiomech.2015.08.015.
- Eilenberg, M.F., Geyer, H., Herr, H., 2010. Control of a powered ankle-foot prosthesis based on a neuromuscular model. IEEE Trans. Neural Syst. Rehabil. Eng. 18 (2), 164–173. https://doi.org/10.1109/TNSRE.2009.2039620.
- Esposito, E.R., Aldridge Whitehead, J.M., Wilken, J.M., 2016. Step-to-step transition work during level and inclined walking using passive and powered ankle-foot prostheses. Prosth. Orthot. Int. 40 (3), 311–319. https://doi.org/10.1177/ 0309364614564021.
- Fallowfield, J.L., Blacker, S.D., Willems, M.E.T., Davey, T., Layden, J., 2012. Neuromuscular and cardiovascular responses of Royal Marine recruits to load carriage in the field. Appl. Ergon. 43 (6), 1131–1137. https://doi.org/10.1016/j.apergo.2012.04.003
- Fey, N.P., Klute, G.K., Neptune, R.R., 2011. The influence of energy storage and return foot stiffness on walking mechanics and muscle activity in below-knee amputees. Clin. Biomech. (Bristol, Avon) 26 (10), 1025–1032. https://doi.org/10.1016/j. clinbiomech.2011.06.007.
- Gailey, R.S., Wenger, M.A., Raya, M., Kirk, N., Erbs, K., Spyropoulos, P., Nash, M.S., 1994. Energy expenditure of trans-tibial amputees during ambulation at self-selected pace. Prosthet. Orthot. Int. 18 (2), 84–91. https://doi.org/10.3109/ 03093649409164389.

- Grimston, S.K., Engsberg, J.R., Kloiber, R., Hanley, D.A., 1991. Bone mass, external loads, and stress fracture in female runners. Int. J. Sport Biomech. 7 (3), 293–302. https://doi.org/10.1123/ijsb.7.3.293.
- Herr, H.M., Grabowski, A.M., 2012. Bionic ankle–foot prosthesis normalizes walking gait for persons with leg amputation. Proc. R. Soc. B Biol. Sci. 279 (1728), 457–464. https://doi.org/10.1098/rspb.2011.1194.
- Hicks, J.L., Uchida, T.K., Seth, A., Rajagopal, A., Delp, S.L., 2015. Is my model good enough? Best practices for verification and validation of musculoskeletal models and simulations of movement. J. Biomech. Eng. 137 (2). https://doi.org/10.1115/ 14020204
- Higginson, J.S., Zajac, F.E., Neptune, R.R., Kautz, S.A., Delp, S.L., 2006. Muscle contributions to support during gait in an individual with post-stroke hemiparesis. J. Biomech. 39 (10), 1769–1777. https://doi.org/10.1016/j.jbiomech.2005.05.032.
- Kern, A.M., Papachatzis, N., Patterson, J.M., Bruening, D.A., Takahashi, K.Z., 2019.
  Ankle and midtarsal joint quasi-stiffness during walking with added mass. PeerJ 7, e7487
- Kim, J., Wensman, J., Colabianchi, N., Gates, D.H., 2021. The influence of powered prostheses on user perspectives, metabolics, and activity: a randomized crossover trial. J. Neuroeng. Rehabil. 18 (1), 49. https://doi.org/10.1186/s12984-021-00842-2
- Klodd, E., Hansen, A., Fatone, S., Edwards, M., 2010. Effects of prosthetic foot forefoot flexibility on gait of unilateral transtibial prosthesis users. J. Rehabil. Res. Dev. 47 (9), 899. https://doi.org/10.1682/JRRD.2009.10.0166.
- Klute, G. K., 2023. Prosthetic Feet. In Foot and Ankle Biomechanics, pp. 749–764. Elsevier. https://doi.org/10.1016/B978-0-12-815449-6.00027-5.
- Knapik, J.J., Reynolds, K.L., Harman, E., 2004. Soldier load carriage: historical, physiological, biomechanical, and medical aspects. Mil. Med. 169 (1), 45–56. https://doi.org/10.7205/MILMED.169.1.45.
- Lamontagne, A., Richards, C.L., Malouin, F., 2000. Coactivation during gait as an adaptive behavior after stroke. J. Electromyogr. Kinesiol. 10 (6), 407–415. https:// doi.org/10.1016/S1050-6411(00)00028-6.
- Latash, M.L., Huang, X., 2015. Neural control of movement stability: Lessons from studies of neurological patients. Neuroscience 301, 39–48. https://doi.org/10.1016/ i.neuroscience.2015.05.075.
- Lefranc, A.S., Klute, G.K., Neptune, R.R., 2024. The influence of load carriage and prosthetic foot type on individual muscle and prosthetic foot contributions to body support and propulsion. J. Biomech. 177, 112379. https://doi.org/10.1016/j. jbiomech.2024.112379.
- Liu, M.Q., Anderson, F.C., Pandy, M.G., Delp, S.L., 2006. Muscles that support the body also modulate forward progression during walking. J. Biomech. 39 (14), 2623–2630. https://doi.org/10.1016/j.jbiomech.2005.08.017.
- McGinnis, K., Snyder-Mackler, L., Flowers, P., Zeni, J., 2013. Dynamic joint stiffness and co-contraction in subjects after total knee arthroplasty. Clin. Biomech. 28 (2), 205–210. https://doi.org/10.1016/j.clinbiomech.2012.11.008.
- McGowan, C.P., Kram, R., Neptune, R.R., 2009. Modulation of leg muscle function in response to altered demand for body support and forward propulsion during walking. J. Biomech. 42 (7), 850–856. https://doi.org/10.1016/j. jbiomech.2009.01.025.

- McGowan, C.P., Neptune, R.R., Clark, D.J., Kautz, S.A., 2010. Modular control of human walking: Adaptations to altered mechanical demands. J. Biomech. 43 (3), 412–419. https://doi.org/10.1016/j.jbiomech.2009.10.009.
- McGowan, C.P., Neptune, R.R., Kram, R., 2008. Independent effects of weight and mass on plantar flexor activity during walking: implications for their contributions to body support and forward propulsion. J. Appl. Physiol. 105 (2), 486–494. https:// doi.org/10.1152/japplohysiol.90448.2008.
- Montgomery, J.R., Grabowski, A.M., 2018. Use of a powered ankle-foot prosthesis reduces the metabolic cost of uphill walking and improves leg work symmetry in people with transtibial amputations. J. R. Soc. Interface 15 (145), 20180442. https://doi.org/10.1098/rsif.2018.0442.
- Moore, I.S., Jones, A.M., Dixon, S.J., 2014. Relationship between metabolic cost and muscular coactivation across running speeds. J. Sci. Med. Sport 17 (6), 671–676. https://doi.org/10.1016/j.jsams.2013.09.014.
- Neptune, R.R., Kautz, S.A., Zajac, F.E., 2001. Contributions of the individual ankle plantar flexors to support, forward progression and swing initiation during walking. J. Biomech. 34 (11), 1387–1398. https://doi.org/10.1016/s0021-9290(01)00105-1.
- Neptune, R.R., McGowan, C.P., 2011. Muscle contributions to whole-body sagittal plane angular momentum during walking. J. Biomech. 44 (1), 6–12. https://doi.org/ 10.1016/j.jbiomech.2010.08.015.
- Neptune, R.R., McGowan, C.P., 2016. Muscle contributions to frontal plane angular momentum during walking. J. Biomech. 49 (13), 2975–2981. https://doi.org/ 10.1016/j.ibiomech.2016.07.016.
- Norvell, D.C., Czerniecki, J.M., Reiber, G.E., Maynard, C., Pecoraro, J.A., Weiss, N.S., 2005. The prevalence of knee pain and symptomatic knee osteoarthritis among veteran traumatic amputees and nonamputees. Arch. Phys. Med. Rehabil. 86 (3), 487–493. https://doi.org/10.1016/j.apmr.2004.04.034.
- Polcyn, A. F., Bensel, C. K., Harman, E. A., Obusek, J. P., Pandorf, C., 2002. Effects of Weight Carried by Soldiers: Combined Analysis of Four Studies on Maximal Performance, Physiology, and Biomechanics.
- Quesada, P.M., Mengelkoch, L.J., Hale, R.C., Simon, S.R., 2000. Biomechanical and metabolic effects of varying backpack loading on simulated marching. Ergonomics 43 (3), 293–309. https://doi.org/10.1080/001401300184413.
- Robinson, R.O., Herzog, W., Nigg, B.M., 1987. Use of force platform variables to quantify the effects of chiropractic manipulation on gait symmetry. J. Manipulative Physiol. Ther. 10 (4), 172–176.
- Rudolph, K.S., Axe, M.J., Snyder-Mackler, L., 2000. Dynamic stability after ACL injury: who can hop? Knee Surg. Sports Traumatol. Arthrosc. 8 (5), 262–269. https://doi. org/10.1007/s001670000130.
- Sanderson, D.J., Martin, P.E., 1997. Lower extremity kinematic and kinetic adaptations in unilateral below-knee amputees during walking. Gait Post. 6 (2), 126–136. https://doi.org/10.1016/S0966-6362(97)01112-0.
- Sasaki, K., Neptune, R.R., 2010. Individual muscle contributions to the axial knee joint contact force during normal walking. J. Biomech. 43 (14), 2780–2784. https://doi. org/10.1016/j.jbiomech.2010.06.011.

- Schnall, B.L., Hendershot, B.D., Bell, J.C., MSE, Wolf, E.J., 2014. Kinematic analysis of males with transtibial amputation carrying military loads. J. Rehabil. Res. Dev. 51 (10), 1505–1514. https://doi.org/10.1682/JRRD.2014.01.0022.
- Schnall, B.L., Wolf, E.J., Bell, J.C., Gambel, J., Bensel, C.K., 2012. Metabolic analysis of male servicemembers with transtibial amputations carrying military loads. J. Rehabil. Res. Dev. 49 (4), 535–544. https://doi.org/10.1682/jrrd.2011.04.0075.
- Seth, A., Hicks, J.L., Uchida, T.K., Habib, A., Dembia, C.L., Dunne, J.J., Ong, C.F., DeMers, M.S., Rajagopal, A., Millard, M., Hamner, S.R., Arnold, E.M., Yong, J.R., Lakshmikanth, S.K., Sherman, M.A., Ku, J.P., Delp, S.L., 2018. OpenSim: Simulating musculoskeletal dynamics and neuromuscular control to study human and animal movement. PLoS Comput. Biol. 14 (7). https://doi.org/10.1371/journal.
- Shamaei, K., Sawicki, G.S., Dollar, A.M., 2013. Estimation of quasi-stiffness and propulsive work of the human ankle in the stance phase of walking. PLoS One 8 (3). https://doi.org/10.1371/journal.pone.0059935.
- Silder, A., Delp, S.L., Besier, T., 2013. Men and women adopt similar walking mechanics and muscle activation patterns during load carriage. J. Biomech. 46 (14), 2522–2528. https://doi.org/10.1016/j.jbiomech.2013.06.020.
- Silverman, A.K., Neptune, R.R., 2012. Muscle and prosthesis contributions to amputee walking mechanics: a modeling study. J. Biomech. 45 (13), 2271–2278. https://doi. org/10.1016/j.jbiomech.2012.06.008.
- Struyf, P.A., van Heugten, C.M., Hitters, M.W., Smeets, R.J., 2009. The prevalence of osteoarthritis of the intact hip and knee among traumatic leg amputees. Arch. Phys. Med. Rehabil. 90 (3), 440–446. https://doi.org/10.1016/j.apmr.2008.08.220.
- Sup, F., Bohara, A., Goldfarb, M., 2008. Design and control of a powered transfemoral prosthesis. Int. J. Robot. Res. 27 (2), 263–273. https://doi.org/10.1177/ 0278364907084588
- Thelen, D.G., 2003. Adjustment of muscle mechanics model parameters to simulate dynamic contractions in older adults. J. Biomech. Eng. 125 (1), 70–77. https://doi. org/10.1115/1.1531112.
- Uchida, T.K., Hicks, J.L., Dembia, C.L., Delp, S.L., 2016. Stretching your energetic budget: how tendon compliance affects the metabolic cost of running. PLoS One 11 (3), e0150378. https://doi.org/10.1371/journal.pone.0150378.
- Umberger, B.R., 2010. Stance and swing phase costs in human walking. J. R. Soc. Interface 7 (50), 1329–1340. https://doi.org/10.1098/rsif.2010.0084.
- Umberger, B.R., Gerritsen, K.G.M., Martin, P.E., 2003. A model of human muscle energy expenditure. Comput. Methods Biomech. Biomed. Eng. 6 (2), 99–111. https://doi. org/10.1080/1025584031000091678.
- Waters, R.L., Perry, J., Antonelli, D., Hislop, H., 1976. Energy cost of walking of amputees: the influence of level of amputation. J. Bone Joint Surg. Am. 58 (1), 42–46
- Winter, D.A., Sienko, S.E., 1988. Biomechanics of below-knee amputee gait. J. Biomech. 21 (5), 361–367. https://doi.org/10.1016/0021-9290(88)90142-X.
- Zmitrewicz, R.J., Neptune, R.R., Sasaki, K., 2007. Mechanical energetic contributions from individual muscles and elastic prosthetic feet during symmetric unilateral transtibial amputee walking: a theoretical study. J. Biomech. 40 (8), 1824–1831. https://doi.org/10.1016/j.jbiomech.2006.07.009.